Numerical Models of Fat Disks: New Scenarios for Fluid Accretion into Black Holes

John F. Hawley
University of Illinois

Larry L. Smarr*
University of Illinois

ABSTRACT

High energy phenomena in astrophysics demand a compact, efficient central engine. The best candidate for this engine is a black hole accreting matter. We briefly review recent descriptions of such accretion flows with emphasis upon the role of numerical calculations in understanding these flows. Certain cases are illustrated using recent numerical computations.

High energy phenomena abound in astronomy, but with few exceptions these phenomenan are not well understood. The most outstanding examples are the quasars. These highly energetic objects have luminosity variations on the order of hours, implying a compact energy source. Another example is the double radio jet emerging from a galaxy core (see Fig. 1). Here also a compact engine is required to power the jets. Since the central regions of quasars and galaxies cannot be observed directly, gaining an understanding of these central engines has not been an easy task.

*Alfred P. Sloan Fellow

One thing astronomers do know is that the amount of energy released in the central regions of quasars can be equivalent to the rest mass energy of up to ten million solar masses. Nuclear energy, which has an efficiency of about 0.8 percent, is inadequate as the source of power. There is, however, another means of releasing energy which can be much more efficient: the release of gravitational binding energy as matter falls into an intense gravitational field. This idea predates that of nuclear power; it was the power source first suggested for a nearby object which is slightly less luminous than a quasar, the sun. A gradual decrease in the sun's radius could provide enough energy to maintain the solar luminosity---but only for about ten million years. The nuclear process proves to be more efficient for the sun but not for a 10^8 solar mass black hole. Given such a deep potential well, gravity power predominates.

Our understanding of gravity as an energy source follows the course by which astronomers came to understand the stellar nuclear burning process. Initially, there were qualitative arguments and "back-of-the-envelope" calculations which demonstrated the feasibility of fusion to power many stages of stellar evolution. Then came numerical calculations involving complex nuclear reaction networks which provided the details as well as producing a few unexpected results. Astrophysicists today have a qualitative picture of the gravity power process, but the details such as the actual net efficiency can be only roughly estimated. Analytic techniques are restricted to the most simplified systems of equations. Clearly numerical calculations are now required.

Consider a most efficient gravity engine, the black hole. The fuel is an external supply of matter, which might be provided by a companion star or surrounding interstellar gas. In the case of a supermassive black hole, entire stars, ripped apart by the intense tidal forces near the hole, could supply matter for accretion. Now, given the gravitational sink and the fuel supply, we must describe the process by which energy is extracted. In the basic analytic scenario, matter orbits the hole in a thin Keplerian disk (see e.g. Shakura and Sunyaev 1973 and Novikov and Thorne 1973). The viscous shear between differentially rotating fluid layers causes a net outward transport of angular momentum, heating the gas as it gradual-

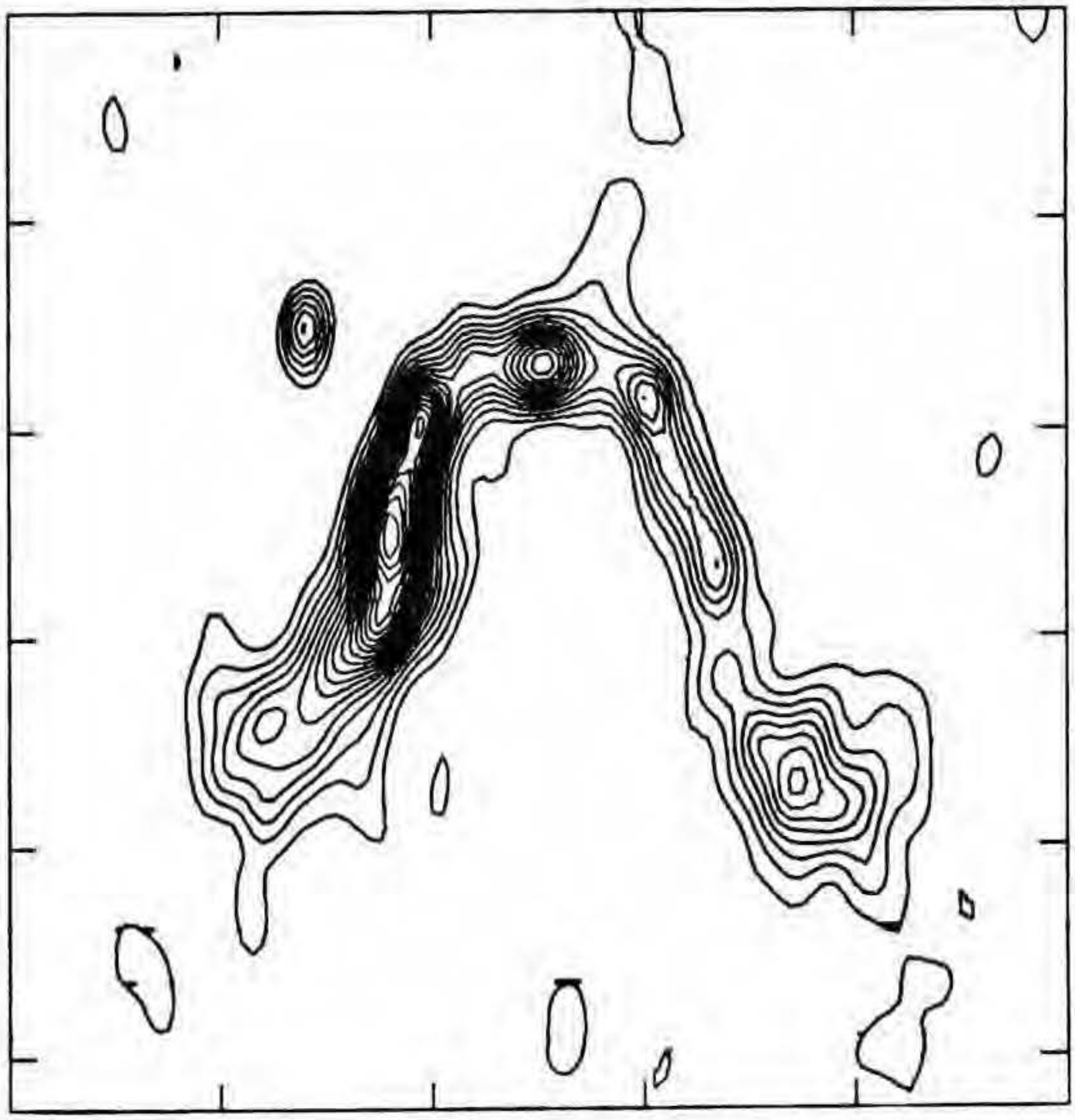


Fig. 1. A contour plot of the radio emission from the double galaxy system Uppsala 7044-7050. The most prominent feature is the double-lobed radio jet emerging from one of the galaxies. Such an energetic phenomenon requires a compact central power source such as an accreting black hole. (Data obtained at the VLA observatory by R. Ekers, L. Smarr and D. Sumi and reduced at the University of Illinois Image Processing System by D. Sumi, Dept. of Astronomy, Univ. of Ill.)

ly spirals in towards the hole. This heat is promptly radiated away at the surface of the disk. Depending on the angular momentum of the hole itself, this process could release anywhere between 5 and 40% of the fluid rest mass energy. High luminosities are achieved by increasing the mass accretion rate. The limit is the "Eddington luminosity" at which the pressure from the radiation is sufficient to disrupt the disk. Assuming that the most energetic quasars radiate at the Eddington limit, a 10^8 solar mass black hole is required to power them.

This analytic picture is quite promising, for it implies that accretion onto black holes could indeed be just the engine needed for observed superluminous objects. The numbers are feasible, but how will accreting matter really behave as it falls in towards the black hole? To answer this we must solve the full general-relativistic equations of hydrodynamics in the gravitational field of the black hole. These equations are so complicated that analytic dynamic calculations are simply not possible. To study the equations numerically we have collaborated with Jim Wilson of Lawrence Livermore National Laboratory (LLNL) in developing a two-dimensional (2-D) general-relativistic hydrodynamic code to simulate fluid flow in the Kerr metric. We assume axisymmetry, an ideal gas equation of state, and a fixed metric to describe the gravitational field.

The first such numerical study was performed at LLNL by Jim Wilson in 1972. He had made considerable progress in generalizing the 1-D fully general-relativistic codes of Michael May and Richard White (1966), to study such phenomena as stellar collapse and supernovae. Drawing upon this experience, he designed a 2-D code to calculate axisymmetric hydrodynamic flows in the fixed Kerr metric, the gravitational field of the black hole; the fluid around the hole is assumed to have negligible mass. Several models were run in which cold material with some angular momentum was allowed to fall towards the hole. One new effect immediately discovered by this work was that shock heating could drastically alter the structure of the flow. Infalling cold fluid with nonzero angular momentum was heated by a standing accretion shock to form dynamically a pressure-supported thick or "fat" disk in which the height of the disk above the equator is comparable to the radial distance from the hole. Instead of a

thin disk, the fluid had formed a non-Keplerian orbiting torus (see Fig. 2). Unfortunately, this pioneering numerical work, published in a short note to the Astrophysical Journal (Wilson 1972), went largely unnoticed.

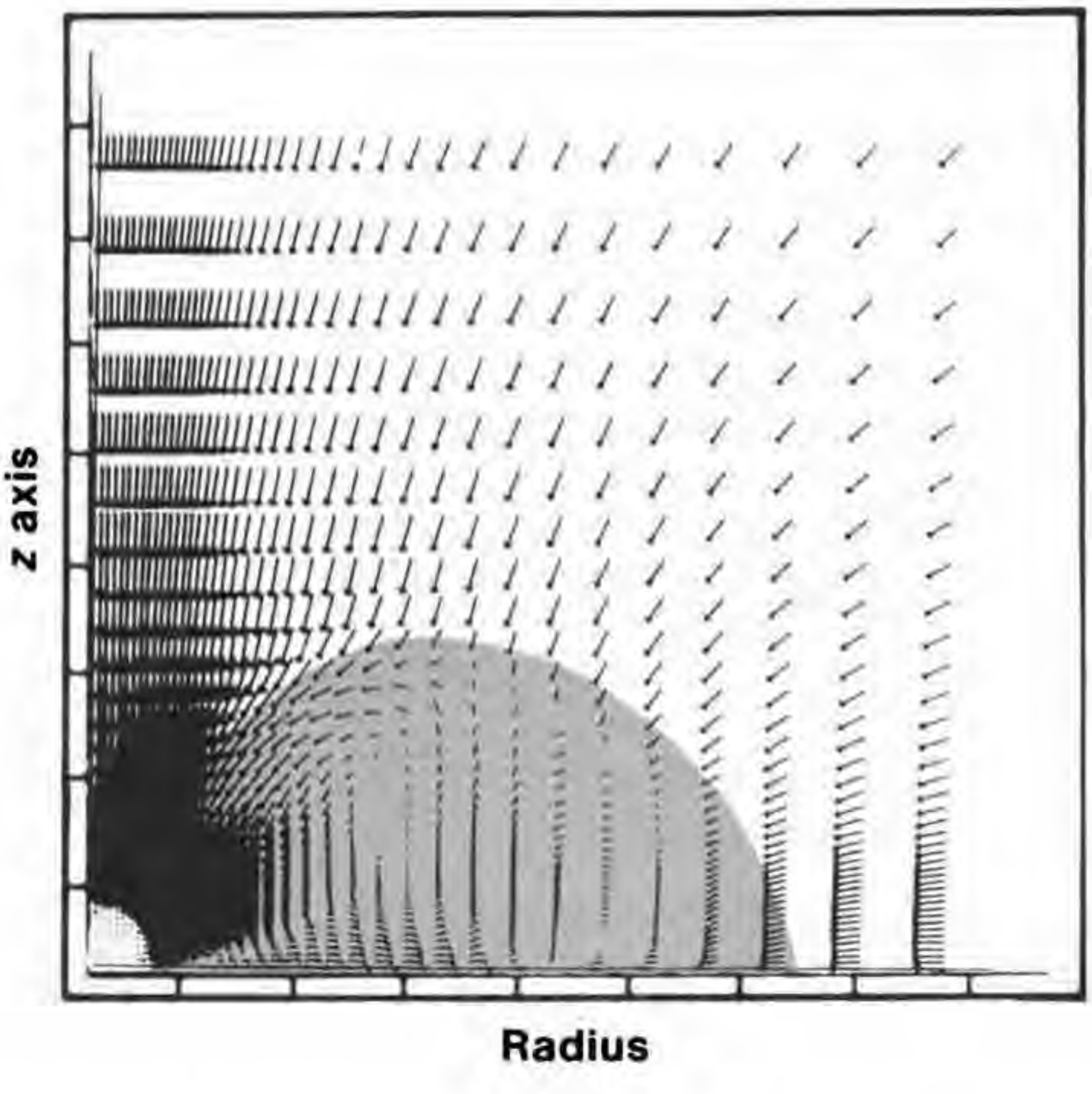


Fig. 2. Infalling cold fluid with nonzero angular momentum shocks and forms a fat disk. The Kerr black hole in this model rotates with the maximum angular momentum (Kerr parameter a = 1). (From Wilson 1972).

In the second half of the seventies the fat disk was rediscovered and considered analytically. Many new and important qualitative features were described, one of the most important of which is a completely general-relativistic effect: in a fat disk, accretion can occur for low angular momentum fluid without viscosity. This

fact was first emphasized in 1976 by B. Paczynski of the Copernicus Astronomical Center in Warsaw (unpublished).

Such accretion can occur because of a fundamental difference between the potential around a black hole and the Newtonian point mass potential. In the Newtonian case, a test particle with nonzero angular momentum will always reach a turning point in its orbit. Further, there is an angular momentum associated with a stable circular orbit for each r, regardless of how close to the origin the orbit is. This is not the case for the general relativistic description of the gravitational field of a black hole. To use the phrase coined by Misner, Thorne and Wheeler (1973), there is a "pit in the potential". Instead of increasing monotonically to infinity as r decreases (the "centrifugal barrier"), the potential turns over and goes to zero at some r outside the horizon (see Fig. 3). That is, in general relativity, the gravitational acceleration always becomes strong enough to overcome centrifugal force. Further, for sufficiently low angular momentum there comes a point where there is no turning radius and no Keplerian circular orbits.

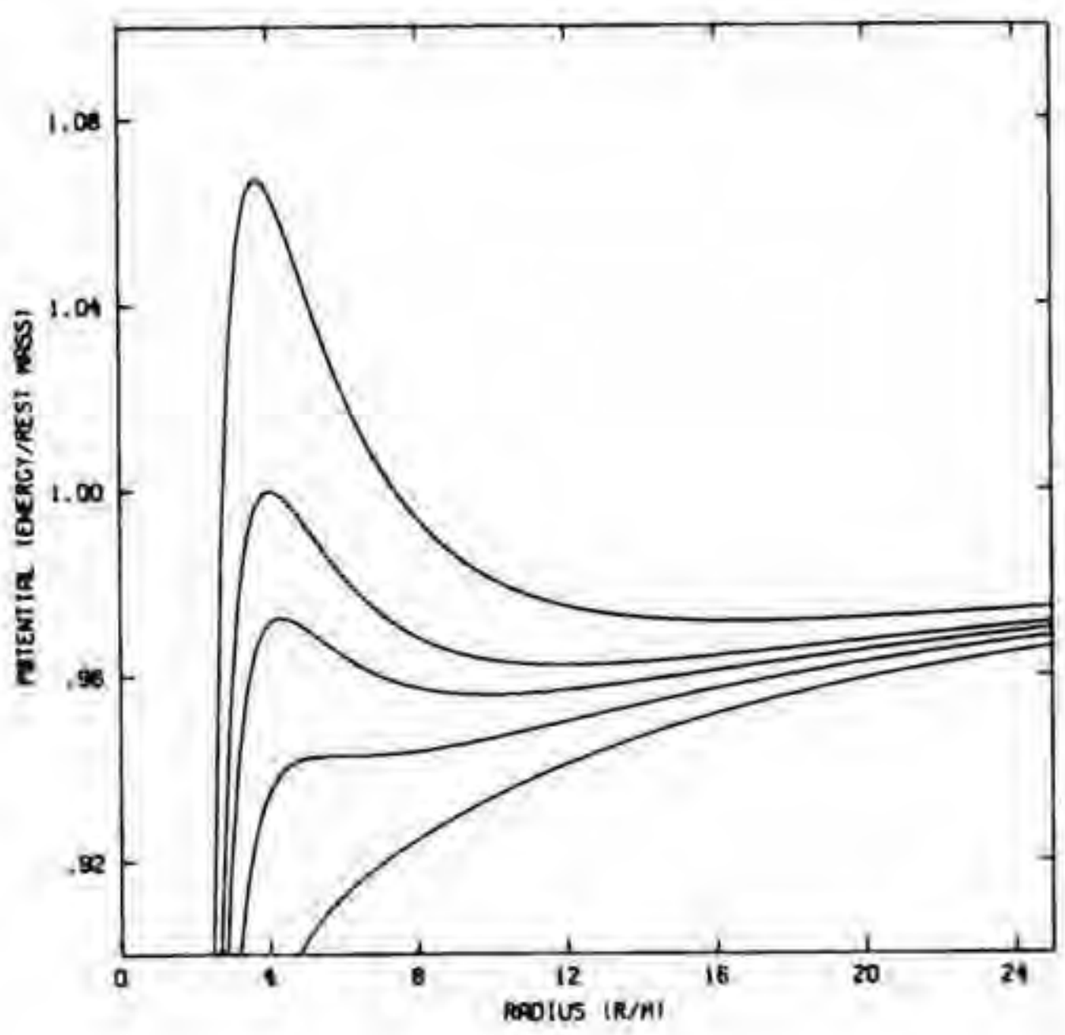


Fig. 3. The effective potential as a function of r along the equator for a Schwarzschild (nonrotating) black hole. From bottom to top the momenta are $\ell = 3.0$, $\ell = \ell_{ms} = 2\sqrt{3}$, $\ell = 3.77$, $\ell = \ell_{mb} = 4.0$ and $\ell = 4.5$. Note the important relativistic effect: the potential does not monotonically increase as r approaches the horizon. There is a "pit in the potential".

For example, the innermost circular orbit for a Schwarzschild (non-rotating) black hole is at $3r_g$, where r_g is the "Schwarzschild radius" of the event horizon. The Schwarzschild radius is given by $r_g = 2M$ where M is the mass of the hole and we have set the gravitational constant G and the speed of light c equal to one. To convert a radial distance to more familiar units, multiply by G/c^2 (= 1.5 kilometers per solar mass). Using this convention, the minimum stable Keplerian orbit for a Schwarzschild hole is at r = 6M. A particle trying to orbit at a smaller radius would spiral rapidly into the hole.

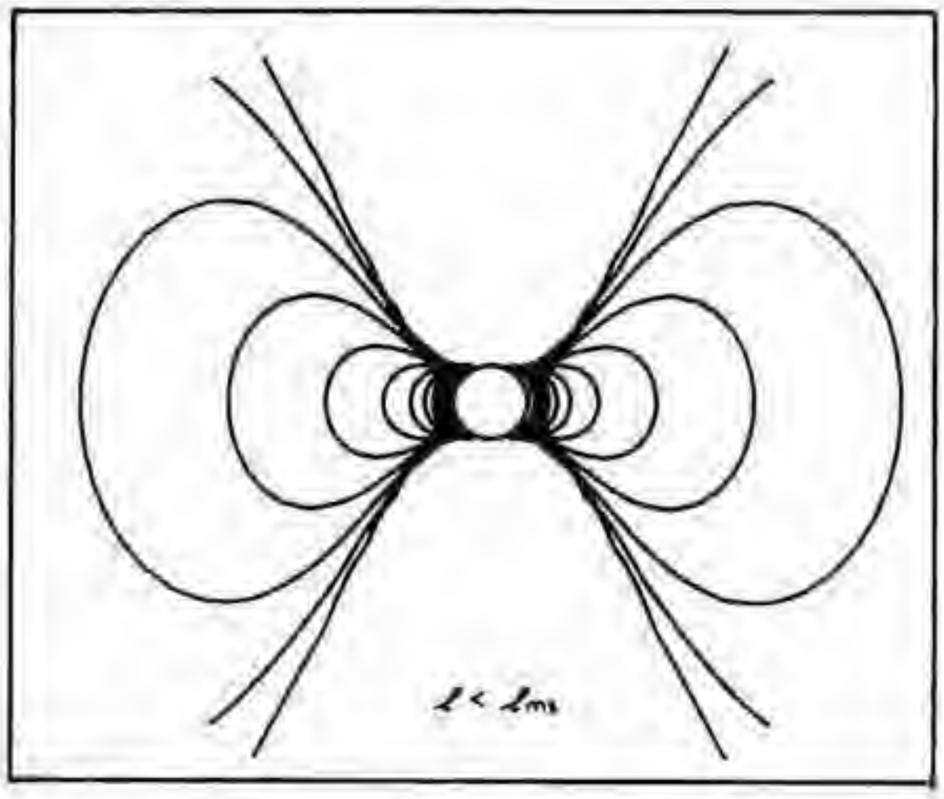
The orbits of test particles in the Kerr metric can be generalized to fluid orbits by defining an angular momentum

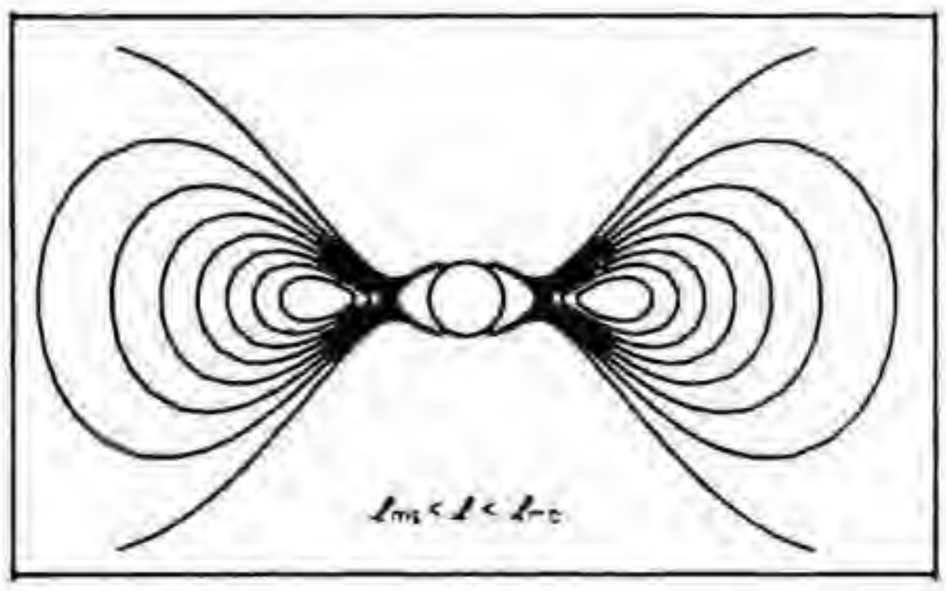
$$\ell \equiv -U_\phi / U_t . \qquad (1)$$

This definition is extremely well suited to the study of fluid flow with nonzero U_ϕ, since in a stationary, axisymmetric flow hU_ϕ and hU_t are separately conserved quantities ($h \equiv$ enthalpy $= 1 + \varepsilon = P/\rho$, where ε = specific internal energy, ρ = baryon density; see Smarr, Taubes, and Wilson 1980 or Hawley, Smarr, and Wilson 1984a for a complete discussion of fluid variables and definitions.) Thus ℓ will be conserved in such flows and can be used to describe fluid orbits in a manner analogous to the test particle case (see Kozlowski et al. 1978, and Bardeen 1973).

As in the test particle case, we can define two critical angular momenta ℓ for a given hole. First, the minimum angular momentum which permits a circular orbit is referred to as ℓ_{ms} ("marginally stable"). Second, the minimum angular momentum for which there is still a turning point in the orbit of a "marginally bound" (energy/rest mass = 1) test particle falling towards the hole from rest at infinity is designated ℓ_{mb}. Any body with $\ell < \ell_{mb}$ which falls from rest at infinity must be captured by the hole. A particle can avoid capture by having less energy than the marginally bound particle, but not if $\ell < \ell_{ms}$. In general, $\ell_{ms} < \ell_{mb}$. For a Schwarzschild hole, $\ell_{ms} = 2\sqrt{3} = 3.46$ (stable orbit at 6M) while $\ell_{mb} = 4.0$ (turning point at 4M).

A diagram such as Figure 3 can be expanded into two spatial dimensions. Figure 4 is an example for a variety of constant angular





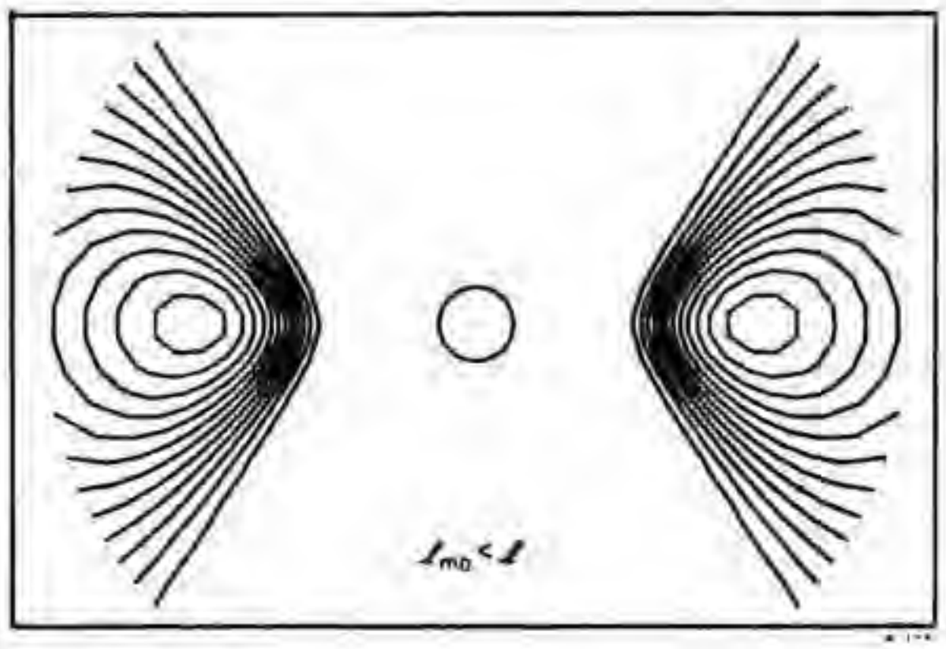


Fig. 4. These figures show surfaces of constant total potential (due to combined gravitational and centrifugal accelerations). They illustrate possible accretion scenarios: a) low angular momentum ($\ell < \ell_{ms}$) potentials are open to the hole and fluid can flow directly in; b) between marginally stable (ℓ_{ms}) and marginally bound (ℓ_{mb}) angular momenta, some potentials end on the hole and some are closed. An accreting disk structure can form; c) for angular momentum larger than ℓ_{mb}, there are stable, pressure-supported disks which remain stable in the absence of viscous dissipation.

moments ℓ. We see that there are surfaces of equal "total potential" determined by the gravitational and centrifugal accelerations. These accelerations can be countered by a pressure force; simply fill the closed potentials with hot fluid. In equilibrium, pressure contours coincide with total potential contours. The pressure maximum will be at the "lowest point" in the potential, which in these examples is at the point of the Keplerian circular orbit for the given angular

momentum (no pressure acceleration is needed to keep a particle at such a point - gravity and centrifugal force exactly cancel!). By changing the angular momentum we can change the equipotential surfaces and consequently the expected fluid behavior.

These features can be quantitatively described by assuming a purely azimuthal, time-stationary, axisymmetric fluid flow with $U^r = U^\theta = 0$ and solving the relativistic Euler equation to derive an equation of force balance (Hawley, et al. 1984a):

$$\nabla P = -\tfrac{1}{2} \frac{S_\alpha S_\beta}{S^t} \partial_i g^{\alpha\beta} \qquad (2)$$

where momentum $S_\alpha = \rho h W U_\alpha$ and W is the relativistic gamma factor. This equation becomes more familiar if we take the weak field Newtonian limit, using

$$ds^2 = -(1 + 2\Phi)dt^2 + (1 - 2\Phi)dr^2 + r^2 d\Omega^2 \qquad (3)$$

to obtain

$$\partial_i P = \rho\left(\tfrac{1}{2} \partial_i (2\Phi) - \tfrac{1}{2}(U_\phi)^2 \partial_i g^{\phi\phi}\right) . \qquad (4)$$

In cylindrical coordinates this is recognized to be the usual Newtonian equations for hydrostatic equilibrium of a nonself-gravitating fluid of angular momentum U_ϕ in a gravitational potential Φ:

$$\frac{\partial P}{\partial R} = \rho\left(\frac{\partial \Phi}{\partial R} + \frac{U_\phi^2}{R^3}\right) ,$$

$$\frac{\partial P}{\partial z} = \rho\left(\frac{\partial \Phi}{\partial z}\right) . \qquad (5)$$

Thus our equation (2) is the fully relativistic equation of hydrostatic equilibrium. Abramowicz et al. (1978) formulate this equation in terms of angular momentum ℓ and angular velocity $\Omega \equiv U^\Phi / U^t$, $(U^r = U^\theta = 0)$:

$$\frac{\nabla P}{\rho h} = -\nabla_i \ln(-U_t) + \frac{\Omega \nabla_i \ell}{1 - \Omega \ell} . \qquad (6)$$

For a disk with a barytropic equation of state $\left(P = P(\rho + \rho\varepsilon)\right)$ the

equipotential surfaces of constant pressure are given by:

$$\psi - \psi_{in} = \ln(-U_t) - \ln(-U_t)_{in} - \int_{\ell_{in}}^{\ell} \frac{\Omega d\ell}{1-\Omega\ell} \quad , \qquad (7)$$

where the subscript "in" refers to the inner equatorial edge of the disk. We consider disks for which ℓ = constant and the surface potential is zero ($hU_t = -1$ throughout the disk). Then equation (7) is simplified to

$$\psi = \ln(-U_t) \qquad (8)$$

and this is employed to describe the equipotential surfaces and the orbits of the fluid flow.

All these ideas lead to modified accretion scenarios. First, fluid falling towards the hole with $\ell < \ell_{mb}$ can be accreted without any additional decrease in angular momentum, since there are always some potential surfaces open to the hole. This provides a new and quite plausible description for the final dynamic infall at the inner edge of an accretion disk, as well as a description of the complete infall process for sufficiently low angular momentum matter. In general, however, fluid away from the hole will have large angular momentum and the accretion of such fluid involves the use of viscosity to decrease ℓ and heat the disk. If this heat is not immediately radiated away, the disk will become hot. This heat will provide a pressure force in the fluid, causing it to puff up away from the equator and fill the equipotential surfaces as described above. In this way a pressure supported fat disk could form from initially cold gas. Angular momentum is transported outward in the disk by the viscous stress, causing ℓ to decrease at the inner edge until it is below the marginally bound value. At this point accretion can be accomplished with no further reduction in ℓ. This tends to reduce the net efficiency of the energy release, since viscous dissipation is not required all the way down to the minimum stable orbit; the subsequent inviscid infall does not efficiently extract the binding energy from the deepest part of the gravitational potential well. On the plus side, however, the fat disk structure can support a larger luminosity: some investigators have estimated that up to 100 times the limit for a thin disk is possible. So, while the

fat disk may be less efficient than a thin disk, given a large enough accretion rate it may be considerably brighter. For detailed discussions of such analytic thick disk models see Abramowicz, et al. (1980), Jaroszyński, et al. (1980), Paczyński and Wiita (1980), Sikora (1981), and Wiita (1982).

Clearly then these new scenarios can have important observational consequences. But analytic analysis of the type done to date, while revealing, cannot say exactly what flows are possible and in what manner they might proceed. How does flow vary with angular momentum? Do structures resembling those described in the equilibrium analytic theory actually develop in hydrodynamic situations? In order to approach these questions in the greater generality permitted by numerical analysis, we have expanded on the original Wilson 1972 study.

From our work, in collaboration with Jim Wilson, we present several examples of calculated inviscid fluid flow in the near hole region. We use a time-explicit, fixed grid Eulerian accretion code with a monotonic transport scheme of Van Leer (1977). To obtain various disk formation models, we introduce fluid on the outer boundary of the finite difference grid with some value of angular momentum ℓ and allow the fluid to flow into the grid. For a complete discussion of the difference techniques used in this code see Hawley, Smarr and Wilson (1984b).

The work we present here is illustrative of the types of flow expected for accreting fluid with nonzero angular momentum. This is essentially an extension of the relativistic "Bondi accretion" solution in which hot fluid with zero angular momentum undergoes steady state radial accretion through a sonic point. The analytic solution for the Bondi flow is given by Michel (1972). As angular momentum is added to the accreting fluid, centrifugal acceleration becomes important, the hydrodynamic equations become analytically untenable, and new accretion phenomena, such as fat disks, become possible.

First consider low angular momentum fluid with $\ell < \ell_{ms}$. For such a fluid there is no orbital turning point; the equipotential surfaces all end on the hole. All the fluid should fall in, and this is indeed what our computer simulation shows. If the outer boundary is continuously resupplied with fluid, a steady-state, non-radial

flow is rapidly established, a flow which in many ways resembles the transonic solution for radial accretion of a hot ideal gas (the "Bondi accretion" solution); such a flow is shown in Figure 5. Now

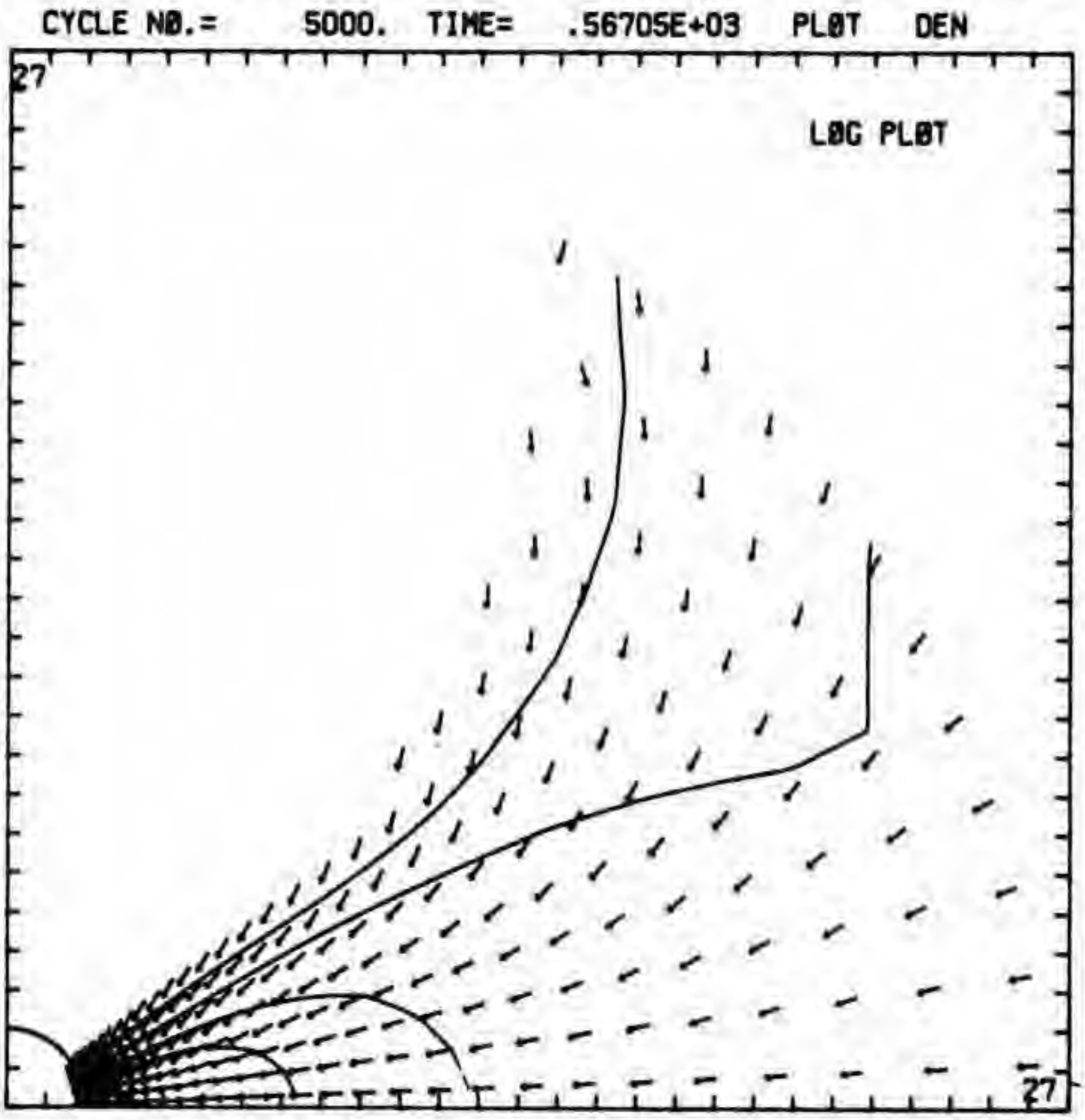


Fig. 5. Density contours and flow directions for a low angular momentum (ℓ = 3.0) accretion model. The contours are logarithmic showing decades in density; the vectors indicate direction of fluid flow, not velocity magnitude. The outer boundary is at 27M in radius. A fluid with angular momentum less than the marginally stable orbit of a black hole (ℓ_{ms}) must fall into the hole on a dynamic timescale. This steady-state solution is the generalization of the Bondi accretion problem to the case of low but nonzero angular momentum.

consider the grid filled with this same low ℓ fluid and do not permit further inflow at the outer boundary. Figure 6 consists of two graphs showing density contours and flow directions at different times for this model. We find that the fluid drains into the hole on an orbital timescale. For our particular value of angular momentum

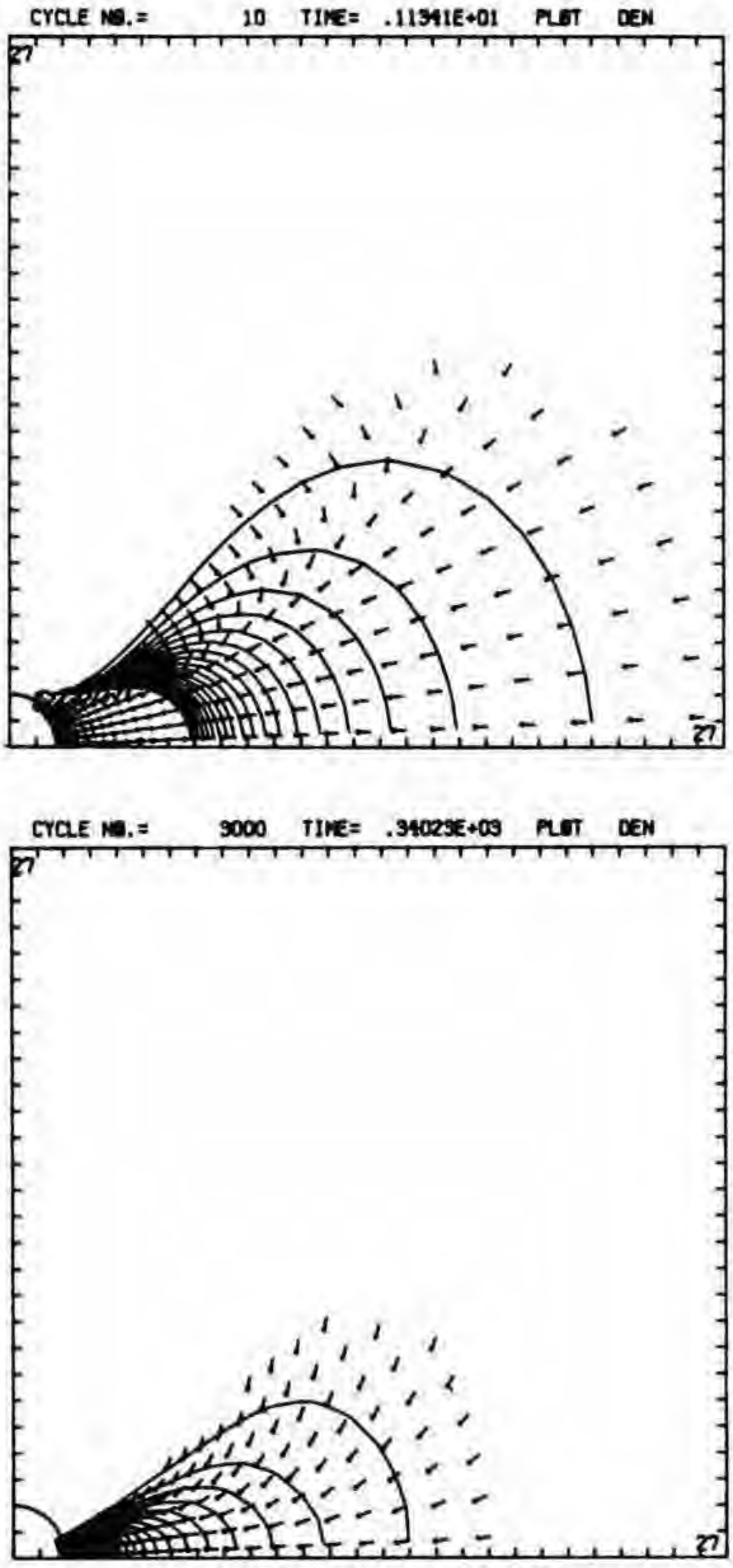


Fig. 6. We begin with $\ell = 3.0$ fluid filling the potential surfaces around a Schwarzschild hole with $U_r = U^\theta = 0$. As the evolution proceeds, gravitational and centrifugal accelerations cause the fluid to spiral into the hole on an orbital timescale.

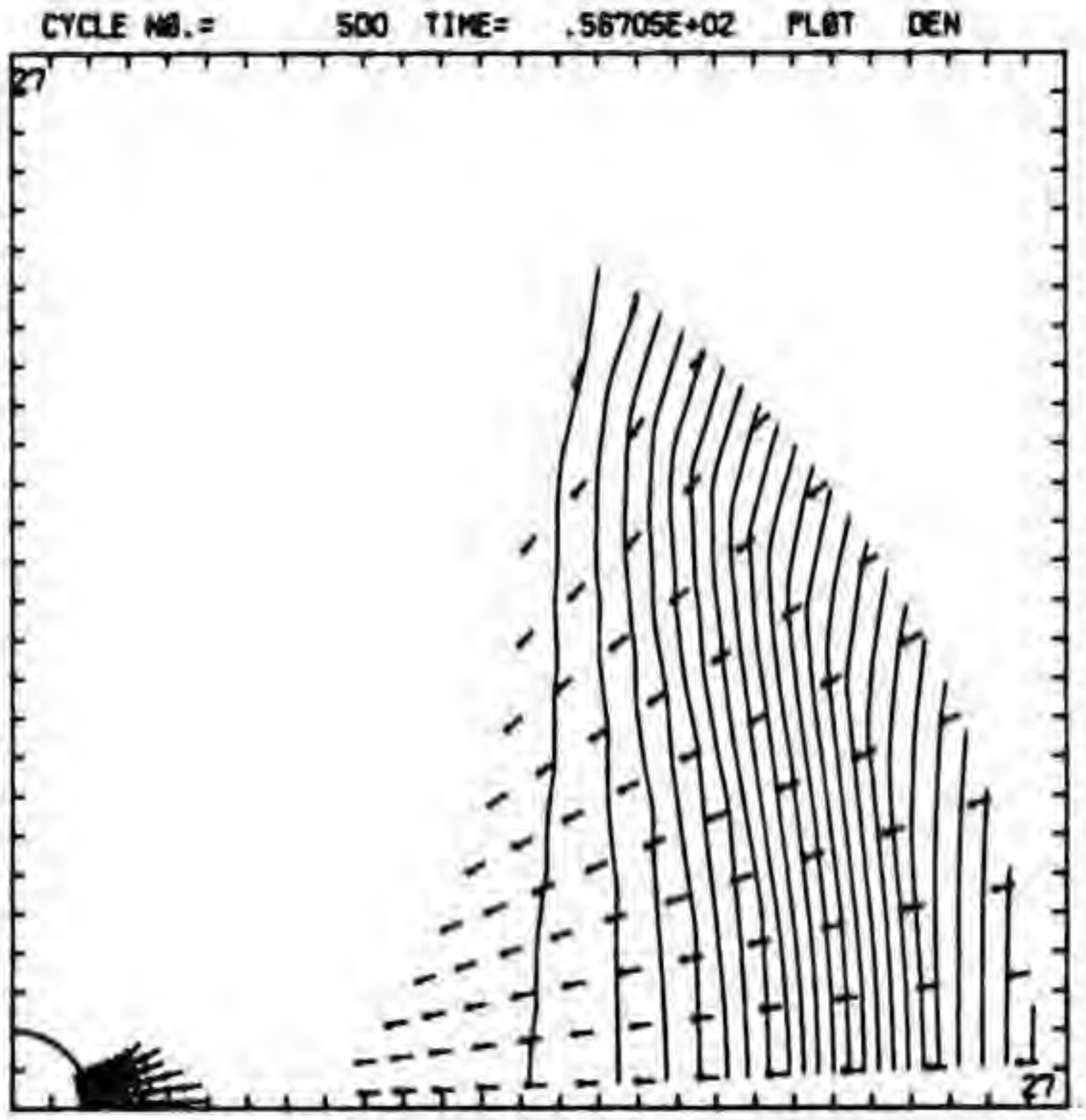
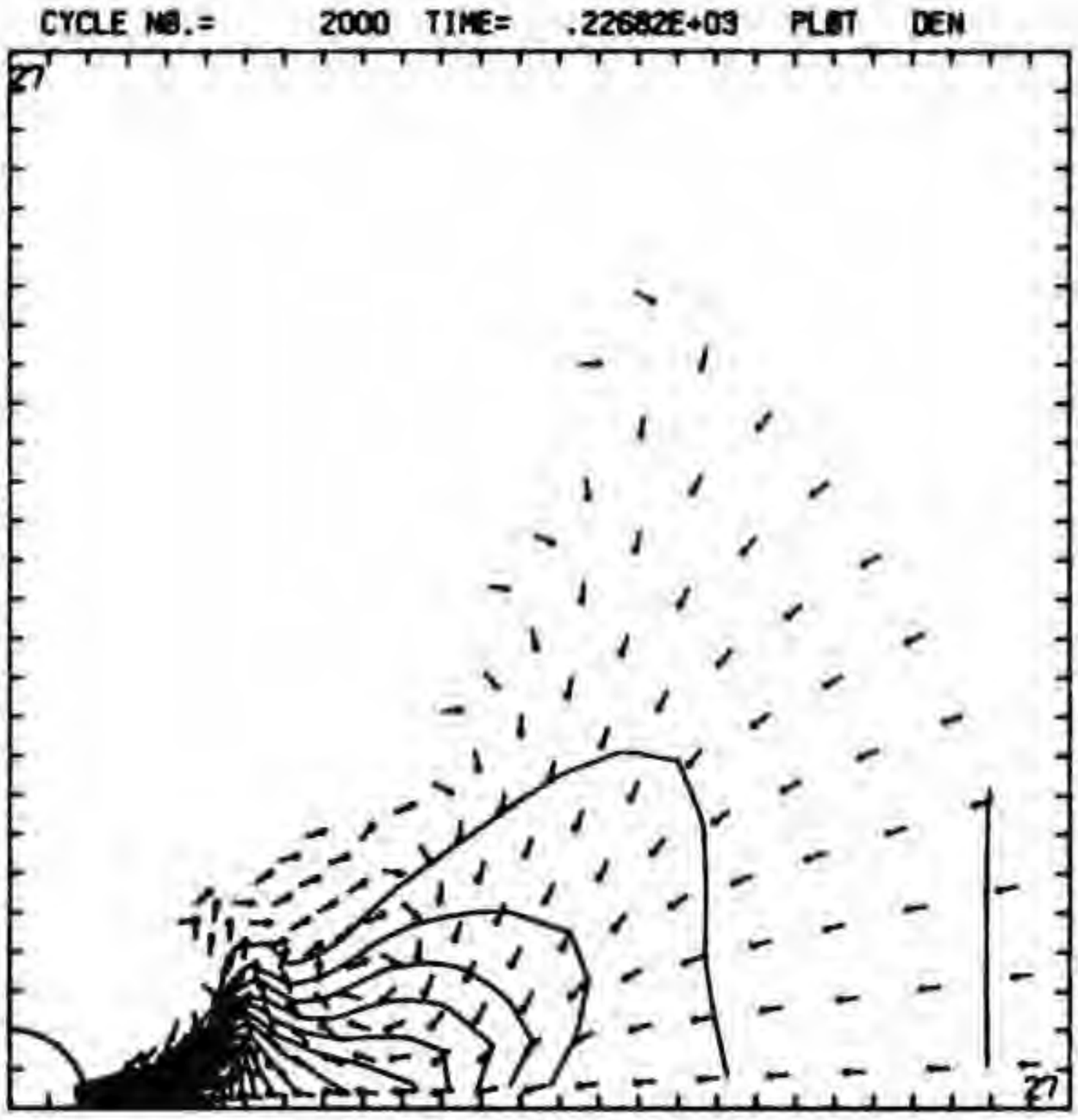


Fig. 7. Fluid with angular momentum ℓ greater than that of the marginally stable orbit flows in from the outer boundary. Much of it "bounces" at a turning radius and a fat disk is dynamically formed with a density and pressure maximum at r = 8m, appropriate for this ℓ = 3.77 disk.



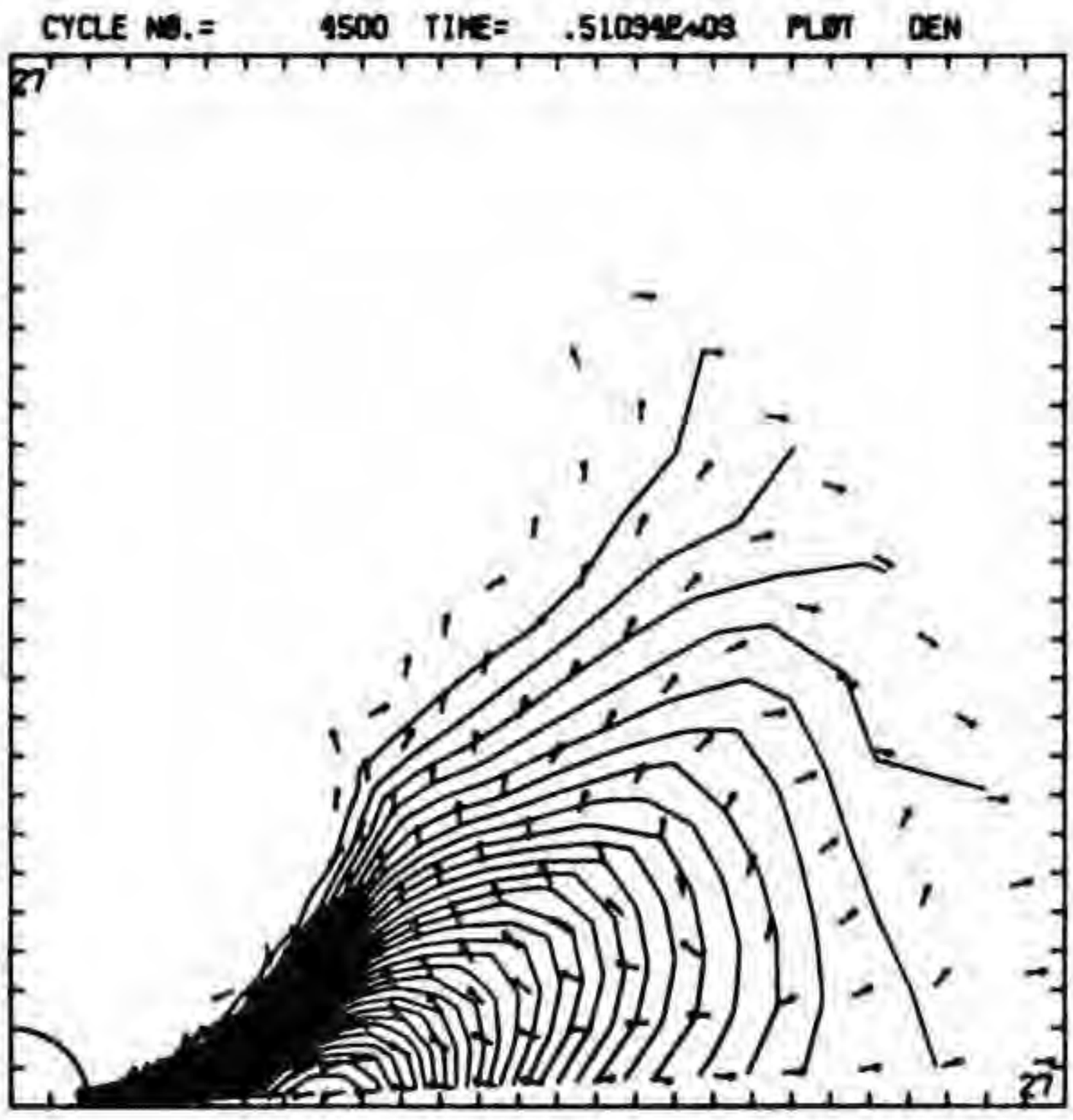


Fig. 7. continued

the orbital period at r = 8M is such that the fluid at that radius has had time to complete 2.4 orbits between the first and secod plot shown in Figure 6. Thus, our calculation verifies that for sufficiently low angular momentum, fluid spirals rapidly into the hole with no viscous shear required.

By increasing the angular momentum slightly to a value $\ell_{ms} < \ell < \ell_{mb}$, we can obtain an entirely new type of behavior in the inflow models. Figure 7 shows a series of plots for such an accretion model. This new behavior is made apparent by referring to Figures 3 and 4. For angular momentum in this range, there is a stable circular orbit and, up to a certain energy, there is also a turning radius. We choose to model a disk with $\ell = 3.77$. For this value of ℓ there is an unstable circular orbit at r = 4.7M on the equator; the stable circular orbit is at r = 8M. The potential surface where $U_t = -0.955$ is the last closed surface; test particles with $-1 < U_t < -0.955$ can be accreted into the hole without encountering a turning point. In the course of our model's evolution we find that a portion of the inflowing fluid "bounces" as it hits an orbital turning point. A region with nonzero circulation forms behind the bounce. Infalling fluid behind begins to fill up the potentials, and gradually a disk forms with a pressure maximum at the predicted point of 8M. A compression wave moves outward and shuts off the inflow at the outer boundary, allowing the density in the disk to drop as fluid continues to drain down the hole. This drop in density permits inflow again and the process repeats itself, though much less dramatically; the disk, once formed, remains, and the maximum density in the disk fluctuates. While the accretion rate at the outer boundary continues to oscillate, the inflow into the hole remains rather steady. The outer boundary inflow rate averages out to about the same as that into the hole (see Fig. 8). Not much significance should be attached to the inflow oscillation at the outer boundary, since it reflects outer boundary conditions, rather than a likely physical phenomenon. However, the relative constancy of the flow into the hole is suggestive. It is quite likely that the potential "nozzle" into the hole can support only a certain maximum flow given an angular momentum and a fluid temperature, much like fluid flow in a nozzle. Since the accretion rate onto the hole in a realistic situation will be determined by factors at large radius away from this nozzle, it is unlike-

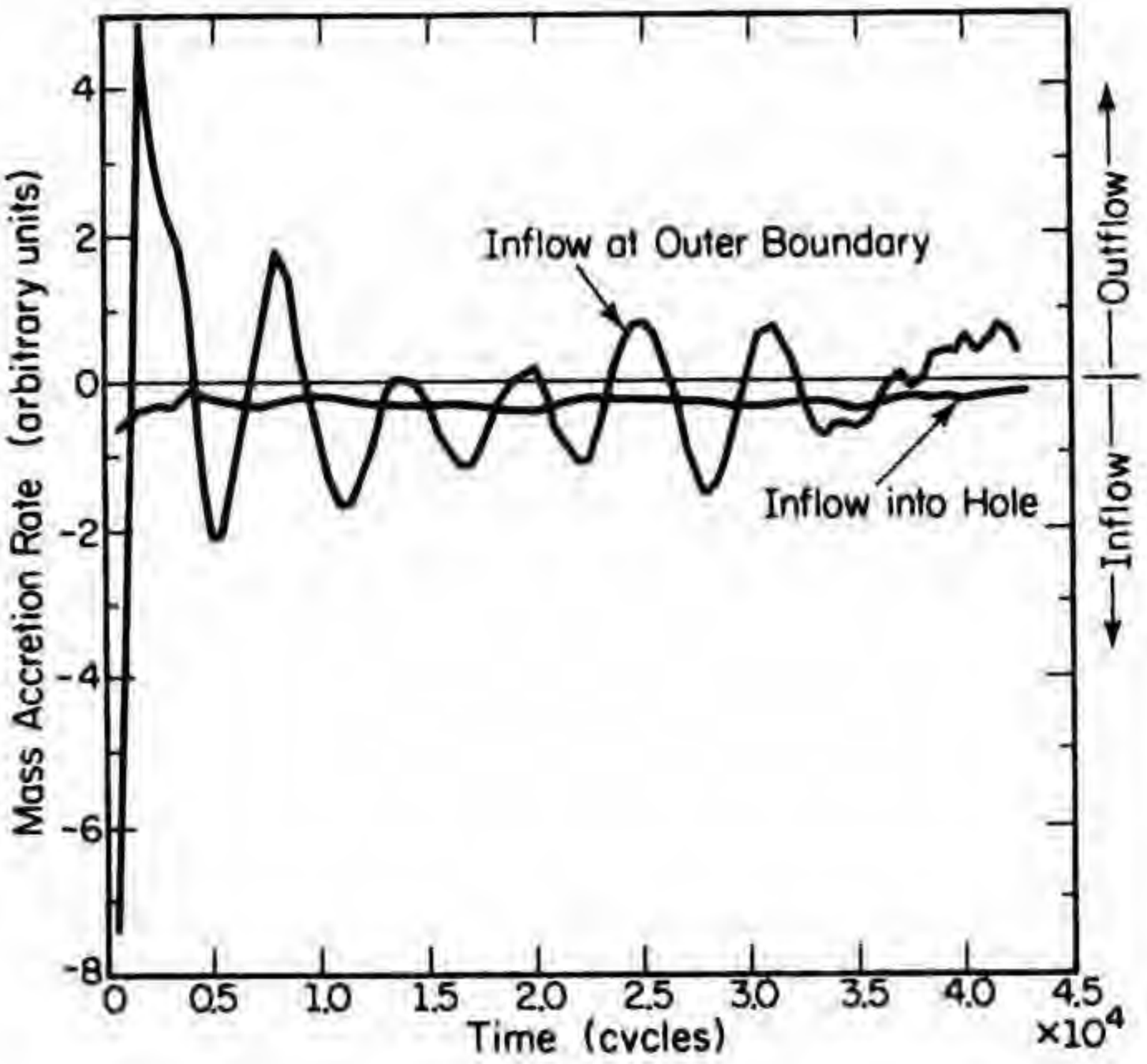


Fig. 8. Mass accretion rate vs. time for the model pictured in Fig. 7. The inflow at the outer boundary is not held fixed and it oscillates in response to dynamic changes in the disk. The inflow into the hole remains constant; the "potential spout" acts like a nozzle and allows only a certain flow rate.

ly that the inflow provided will just match the rate supported by the nozzle. A smooth, steady state flow may not be a likely scenario; a completely dynamic time-dependent flow may well be required.

To examine this nozzle scenario further we can assume a steady state flow and use Bernoulli's equation to calculate the accretion rate through the nozzle. This was first done by Kozlowski et al. (1978), who used enough assumptions to enable them to obtain a completely analytic solution for $\dot{M}$. We numerically integrate the equations in order to obtain greater generality in our results.

We begin with Bernoulli's equation

$$hU_t = \text{constant} = -1 \qquad (9)$$

assuming marginally bound fluid and consequently a disk surface potential equal to zero. Next we select a sonic point inside the nozzle; such a choice, along with the assumption that the flow is purely radial, completely determines the accretion rate for a given value of ℓ. Kozłowski et al. assume that the sonic point occurs at the radius of the cusp in the potential (the unstable circular orbit see Fig. 9), here $r_c = 4.7$ M. Our numerical models for this disk indicate that a sonic point occurs at $r_s = 4.3$ M. Trying both values, we compute $U_t(\theta)$ out to the disk surface at θ_m where $U_t = -1$. Using ℓ = constant, $U_\theta = 0$ and velocity renormalization, we obtain

$$U_t^2 \, (g^{tt} - 2g^{t\phi}\ell + g^{\phi\phi}\ell^2) = -(1 + g^{rr}U_r^2) \; . \qquad (10)$$

Then using Bernoulli's equation and assuming

$$U^r = V_{sound} = \left(\frac{\Gamma(\Gamma-1)\varepsilon}{h}\right)^{1/2} \qquad (11)$$

for an ideal gas, we obtain a quadratic equation for specific internal energy ε. This yields the mass flux $\rho U^r\sqrt{-g}$ at that angle θ. This flux is numerically integrated from $\pi/2$ to θ_m to obtain the total accretion rate.

In Figure 9 the results of this calculation for an $\ell = 3.77$ fluid are displayed along with the mass flux into the hole in our numerical model. This figure shows that Bernoulli's equation yields a value comparable with the average accretion rate for the numerical model. The oscillations in the model's rate are driven by oscillations in the disk as a whole (and hence by the flow at the outer boundary), not by a change in the position of the sonic point.

These results are meant to be suggestive only. The numerical grid in this model is too coarse to allow us to draw conclusions in detail. However, the following qualitative statements can be made. 1) For fat disks with $\ell_{ms} < \ell < \ell_{mb}$, some rate of accretion over the potential cusp and into the hole can be supported. 2) In such an

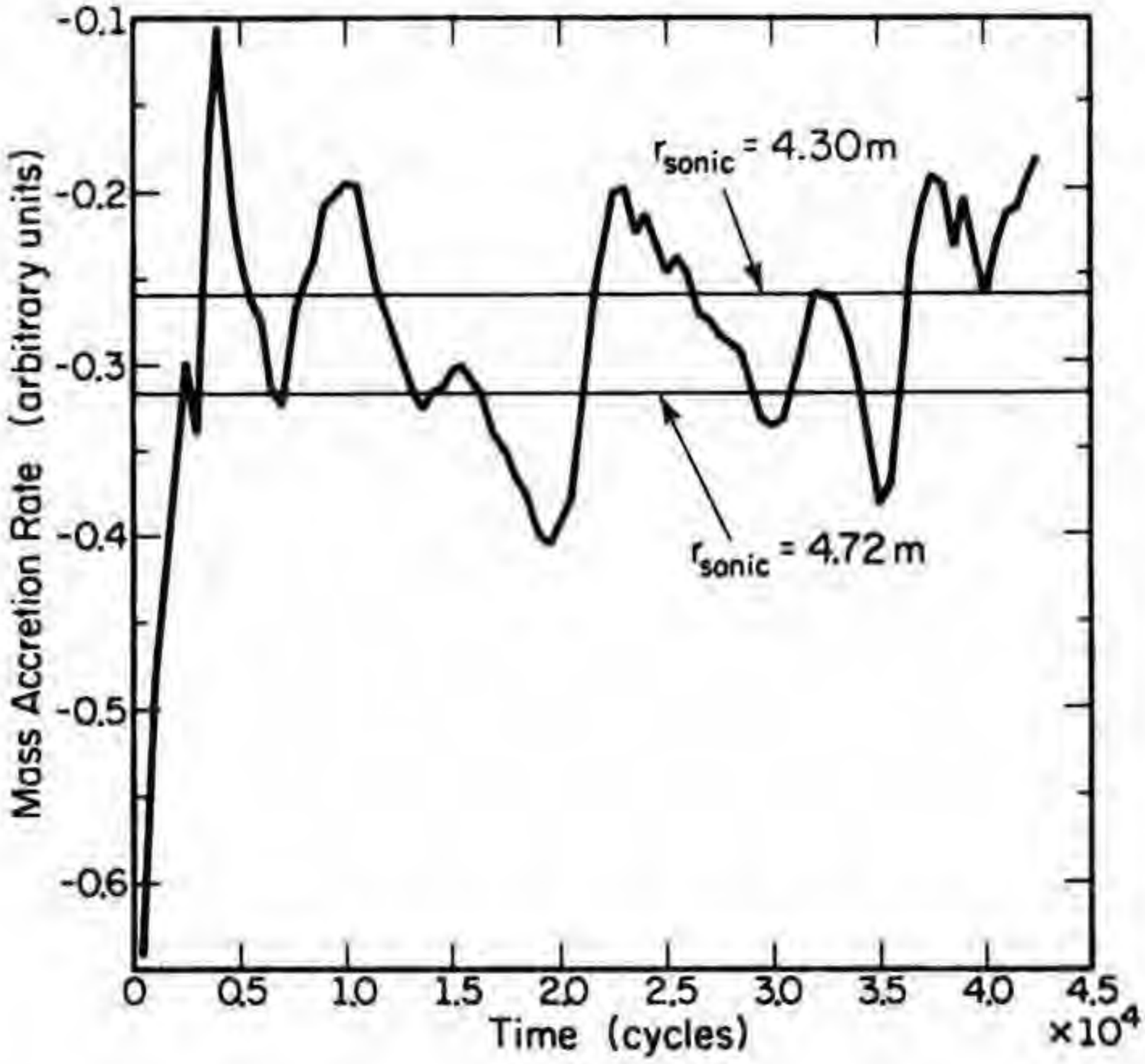


Fig. 9. Numerically calculated inflow into the hole for the ℓ = 3.77 model is displayed along with the inflow values for two sonic points r_s = 4.3 M. and r_s = 4.7 M. = r_c as calculated using the Bernoulli equation analysis. The analytic value is comparable to the average numerical accretion rate.

accretion flow, the sonic point occurs in the nozzle within the radius of the potential cusp. 3) The flow in the disk itself is subsonic, possibly supporting large-scale circulation. 4) The accretion rate into the hole can be approximated using Bernoulli's equation and treating the flow inside the nozzle as radial transonic fluid flow with constant angular momentum.

If we increase the angular momentum of the infalling fluid, we obtain the especially simple case of $\ell > \ell_{mb}$. For this angular momentum, none of the potential surfaces end on the hole; a stationary, pressure-supported, axisymmetric fat disk can be completely

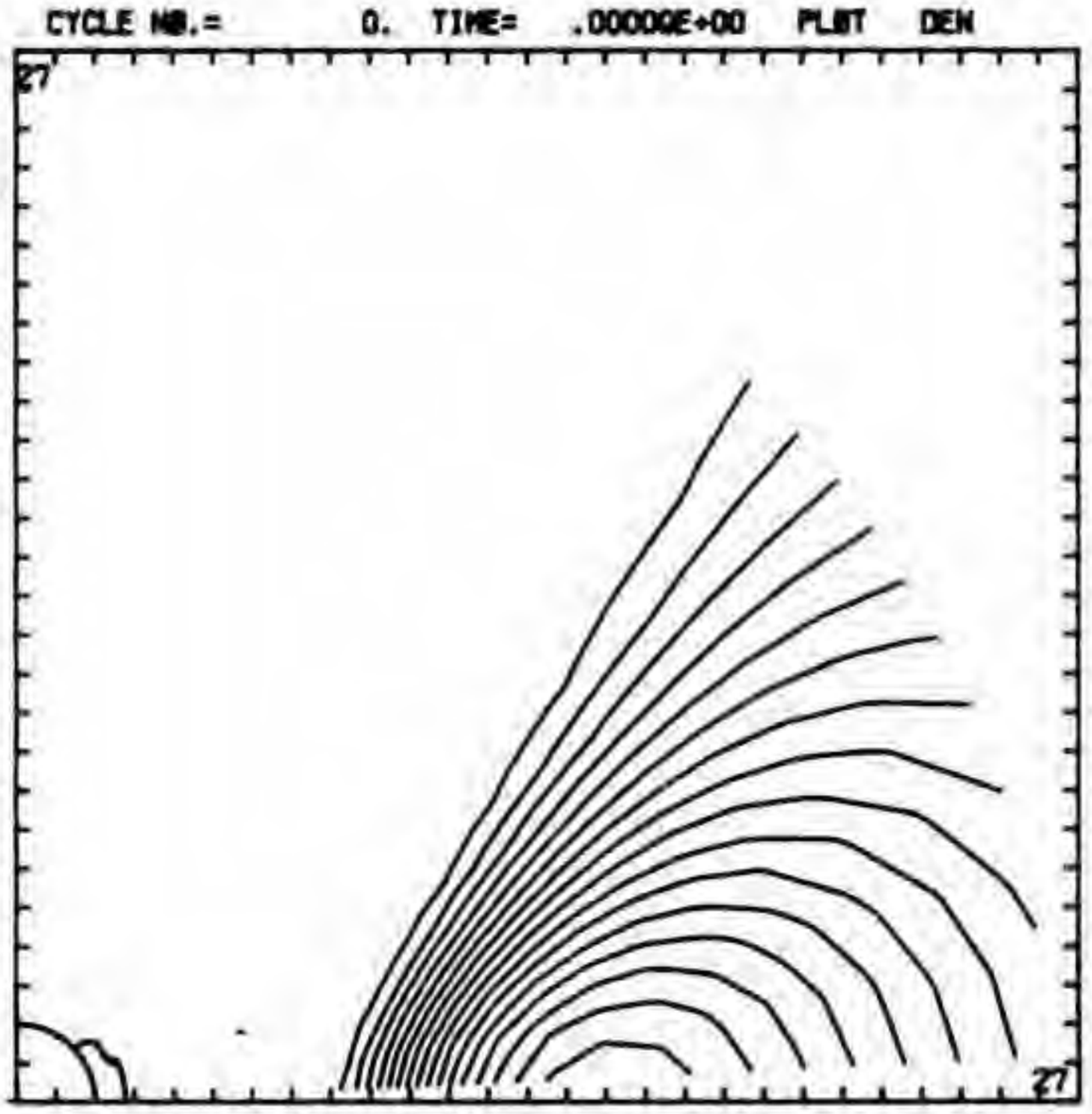


Fig. 10. For sufficiently high angular momentum, one can form a stable, pressure-supported fat disk which remains in equilibrium in the absence of dissipative forces.

specified analytically. The inner portion of such a disk is shown in Figure 10. For this disk some viscosity would be necessary to redistribute the angular momentum in order to permit accretion. In addition to being an interesting solution of the hydro equations, a model of this disk also serves the practical purpose of providing a code test. To maintain a stationary solution with a finite difference code, the various computed accelerations in both dimensions must repeatedly cancel. Such a test, combined with an ensemble of others, serves to calibrate the code and permit proper evaluation of results.

From this work we can conclude that the dynamic flow of a hot fluid with angular momentum tends naturally to form a fat disk structure and that the final accretion onto the hole is likely to proceed on dynamic freefall rather than viscous timescales once the angular momentum has dropped below ℓ_{mb}. Future work will include the magnetohydrodynamic equations to study the important effects of magnetic fields in the disk. Radiation and viscosity have obvious importance, and efforts to include those terms are also under way.

This work is but the beginning of attempts to understand the hydrodynamics of fat disks and many of our results are preliminary. The advent of supercomputers and advanced numerical hydrodynamic techniques have finally made possible the necessary studies. There is every reason to expect that our understanding of these accretion scenarios will soon increase manyfold.

Partial support for this work was provided by the National Science Foundation through grant PHY80-01496 and by the Department of Energy. The National Center for Atmospheric Research is acknowledged as the source for the graphics software. Computational work was performed on the University of Illinois Cyber 175 and the VAX and Image Processing System, operated jointly by the departments of Astronomy and Atmospheric Science and the Computer Services Office. One of us (JH) wishes to thank Martin Rees and Mitch Begelman for enlightening discussions and the Institute of Astronomy, Cambridge, UK for its hospitality. Finally we thank Joan Centrella, Mike Norman, and K.-H. Winkler for many illuminating discussions on code differencing and testing.

REFERENCES

Abramowicz, M.A., Jaroszyński, M., and Sikora, M. 1978, Astr. Ap., **63**, 221.

Abramowicz, M., Calvani, M., and Nobili, L. 1980, Ap. J., **242**, 772.

Bardeen, J.M. 1973, in "Black Holes" ed. B. DeWitt and C. DeWitt (New York: Gordon and Breach).

Hawley, J.F., Smarr, L.L., and Wilson, J.R. 1984a, Ap. J., **277**, 296.

_____. 1984b, Ap. J. Suppl., **55**, 211.

Jaroszyński, M., M., Abramowicz, M., and Paczyński, B. 1980, Acta. Astr., **30**, 1.

Kozłowski, M., Jaroszyński, M., and Abramowicz, M.A. 1978, Astr., **63**, 209.

May, M.M., and White, R.H. 1966, Phys. Rev., **141**, 1232.

Michel, F.C. 1972, Astr. Sp. Sci., **15**, 153.

Misner, C.W., Thorne, K.S., and Wheeler, J.A. 1973, "Gravitation" (San Francisco: W-H Freeman and Co.).

Novikov, I., and Thorne, K.S. 1973, in "Black Holes" ed. B. DeWitt and C. DeWitt (New York: Gordon and Breach).

Paczyński, B., and Wiita, P.J. 1980, Astr. Ap., **88**, 23.

Shakura, N.I., and Sunyaev, R.A. 1973, Astr. Ap., **24**, 337.

Sikora, M. 1980, M.N.R.A.S., **196**, 257.

Smarr, L.L., Taubs, C., and Wilson, J.R. 1980, from "Essays in General Relativity", ed. F.J. Tipler (New York: Academic Press.)

Van Leer, B. 1977, J. Comp. Phys., **23**, 276.

Wiita, P.J. 1982, Ap. J., **256**, 666.

Wilson, J.R. 1972, Ap. J., **173**, 431.